DMD #18382

THE INFLUENCE OF CYP3A5 EXPRESSION ON THE EXTENT

OF HEPATIC CYP3A INHIBITION

IS SUBSTRATE-DEPENDENT: AN *IN VITRO-IN VIVO* EVALUATION

Nina Isoherranen, Shana R. Ludington, Raymond C. Givens, Jatinder K. Lamba, Susan N. Pusek, E. Claire Dees, David K. Blough, Kazunori Iwanaga, Roy L. Hawke, Erin G. Schuetz, Paul B. Watkins, Kenneth E. Thummel, and Mary F. Paine

Departments of Pharmaceutics (N.I., K.I., K.E.T.) and Pharmacy (D.K.B.), School of Pharmacy, University of Washington, Seattle, WA; Division of Pharmacotherapy and Experimental Therapeutics, School of Pharmacy (S.R.L., R.L.H., M.F.P.), General Clinical Research Center (R.C.G., S.N.P., P.B.W.), and Department of Medicine (E.C.D., P.B.W.), University of North Carolina, Chapel Hill, NC; Department of Pharmaceutical Sciences, St Jude Children's Research Hospital, Memphis, TN (J.K.L., E.G.S.).

Running title: CYP3A5 expression influences the extent of CYP3A inhibition

Corresponding author:

Mary F. Paine

3312 Kerr Hall, CB#7360

School of Pharmacy

The University of North Carolina at Chapel Hill

Chapel Hill, NC 27599-7360

Office: (919) 966-9984

Fax: (919) 962-0644

Email: mpaine@med.unc.edu

Number of . . .

Text pages: 29

Tables: 2

Figures: 5

References: 39

Words in *Abstract*: 240

Words in *Introduction*: 739

Words in *Discussion*: 1459

Abbreviations: HLM, human liver microsomes; rCYP3A, recombinant CYP3A; PVDF, polyvinylidene difluoride; ERMBT, erythromycin breath test

ABSTRACT

Despite several studies suggesting that CYP3A5 expression can influence the extent of hepatic CYP3A-mediated inhibition, a systematic *in vitro-in vivo* evaluation of this potential clinically important issue has not been reported. Using representative probes from two distinct CYP3A substrate subgroups (midazolam, erythromycin), the inhibitory potency of fluconazole was evaluated in pooled human liver microsomes (HLM) with a low or high specific CYP3A5 content, in recombinant CYP3A enzymes (rCYP3As), and in healthy volunteers lacking or carrying the *CYP3A5*1* allele. Fluconazole was a slightly more potent inhibitor of CYP3A activity in CYP3A5- HLM than in CYP3A5+ HLM with midazolam (K_i of 15 µM and 25 µM, respectively), but not with erythromycin (IC_{50} of 71 µM and 53 µM, respectively). In comparison, fluconazole was a much more potent inhibitor of rCYP3A4 than rCYP3A5 with both midazolam (K_i of 7.7 µM and 54 µM, respectively) and erythromycin (IC_{50} of 100 µM and 350 µM, respectively). As predicted from HLM, with intravenous midazolam, the average ($\pm$SD) *in vivo* K_i ($K_{i,iv}$) was significantly higher in *CYP3A5*1* carriers (24 ± 17 µM and 17 ± 8 µM for homozygous and heterozygous groups, respectively) than in noncarriers (13 ± 6 µM) (p=0.02). With the erythromycin breath test, the average $K_{i,iv}$ was not different between homozygous *CYP3A5*1* carriers (30 ± 12 µM) and noncarriers (58 ± 53 µM). In conclusion, the effect of CYP3A5 on hepatic CYP3A-mediated inhibitory drug-drug interactions is substrate-dependent, and HLM, rather than rCYP3As, are the preferred *in vitro* system for predicting these interactions *in vivo*.

INTRODUCTION

Adverse interactions between two or more medications have been a longstanding problem in clinical practice. Such interactions frequently result from one drug impairing the elimination of another, which can lead to increased systemic concentrations of the affected drug and the potential for an adverse or toxic reaction. The cytochrome P450 3A (CYP3A) subfamily, consisting primarily of CYP3A4 and CYP3A5 in adults, is believed to participate in the metabolism of over half of therapeutic agents that undergo oxidation (Wilkinson, 2005). Taken together, inhibition of CYP3A-mediated metabolism is a common mechanism underlying numerous drug-drug interactions. In addition, the extent of inhibition of CYP3A-mediated drug clearance by a co-medicant often varies between individuals, making it difficult to predict the magnitude and severity of the interaction.

Both CYP3A4 and CYP3A5 are expressed primarily in the liver and small intestine. Although >30 allelic variants in the *CYP3A4* gene have been identified, low variant frequencies, often combined with a lack of functional consequence, indicate a limited contribution by these variants to the large interindividual variation observed in CYP3A4 expression (Lamba *et al.*, 2002; Wojnowski, 2004). In contrast, CYP3A5 expression is clearly polymorphic, and the frequency of robust expression of a functionally significant protein results from genetic mutations that vary among different ethnic groups (Lamba *et al.*, 2002; Xie *et al.*, 2004). For example, CYP3A5 protein has been detected readily in liver specimens obtained from 10-40% of various European and North American Caucasian individuals, 33% of Japanese individuals, and 55% of African Americans (Lamba *et al.*, 2002). Although CYP3A4 generally represents the dominant CYP3A enzyme in the liver, CYP3A5 can represent more than 50% of total hepatic CYP3A content in some individuals (Kuehl *et al.*, 2001; Lin *et al.*, 2002).

Inheritance of at least one copy of the reference *CYP3A5* allele (*CYP3A5*1*) confers CYP3A5 expression, whereas inheritance of two copies of a variant allele (*CYP3A5*3*) confers undetectable or very low CYP3A5 expression (Kuehl *et al.*, 2001). Consistent with the varying

frequencies of CYP3A5 expression, the frequency of *CYP3A5*3* ranges from 85-95% in Caucasians, from 65-85% in Chinese and Japanese individuals, and from 27-55% in African Americans (Lamba *et al.*, 2002; Xie *et al.*, 2004). In addition to *CYP3A5*3*, two other variants, *CYP3A5*6* and *CYP3A5*7*, are associated with reduced CYP3A5 expression and are more common in individuals of African origin (2-17%) compared to Caucasians and Asians (<2%) (Lamba *et al.*, 2002; Xie *et al.*, 2004). Accordingly, all three variants should be considered in any genotyping-based prediction of CYP3A5 function in populations of African origin (Hustert *et al.*, 2001).

CYP3A4 and CYP3A5 share most of the same substrates (Huang *et al.*, 2004), and *in vitro* investigations have indicated that CYP3A5 can be less susceptible to inhibition than CYP3A4. Early examples involved the antifungal agents ketoconazole and fluconazole (Gibbs *et al.*, 1999). Using recombinant CYP3A enzymes and midazolam as the substrate, the K_i of ketoconazole towards CYP3A5 was fourfold greater than that towards CYP3A4 (110 *vs.* 27 nM); an even greater difference was observed for fluconazole (85 *vs.* 9 µM). A weaker inhibitory potency toward CYP3A5 compared to CYP3A4 was reported subsequently for other clinically relevant inhibitors including diltiazem, nicardipine, and mifepristone (Jones *et al.*, 1999; McConn *et al.*, 2004). These observations suggest that genotypic differences in susceptibility to CYP3A inhibition could explain in part the large interindividual variation in the extent of inhibition of drug clearance by drugs and other xenobiotics.

A caveat to the aforementioned inhibitory differences between the CYP3As is that only midazolam was used as the CYP3A probe. *In vitro* evidence suggests that the extent of inhibition of CYP3A activity varies with substrate (Kenworthy *et al.*, 1999; Stresser *et al.*, 2000; Wang R *et al.*, 2000). This variation is explained in part, at least for CYP3A4, by the existence of multiple binding domains within the enzyme active site (Hosea *et al.*, 2000; Schrag and Wienkers, 2001). Midazolam, testosterone, and nifedipine appear to bind to different domains and are representative of three distinct substrate subgroups (Kenworthy *et al.*, 1999). The use

of at least two representative CYP3A substrates has been recommended for both the *in vitro* and *in vivo* evaluation of the inhibitory potential of drugs and other xenobiotics (Kenworthy *et al.*, 1999; Yuan *et al.*, 2002).

To our knowledge, a systematic *in vitro-in vivo* correlation regarding inhibitor potency towards different CYP3A substrates in humans with different CYP3A5 genotypes has not been evaluated. Accordingly, the objectives of the current work were to determine the inhibitory potency of fluconazole towards two distinct probe substrates using pooled HLM with known CYP3A5 protein content and in healthy volunteers with known *CYP3A5* genotype. Midazolam and erythromycin were selected as the substrates because both can be given safely and intravenously to humans. Fluconazole was selected as the inhibitor based on the 9-fold difference in inhibitory potency between recombinant CYP3As (Gibbs *et al.*, 1999); minimal plasma protein binding; metabolism representing a minor route of elimination; a lack of effect on the efflux transporter P-glycoprotein (Venkatakrishnan *et al.*, 2000); and a long elimination half-life *in vivo* (~30 hrs), which would provide a relatively stable concentration during the period of substrate elimination.

METHODS

Materials and chemicals

Western blotting reagents and materials (sodium dodecyl sulfate, acrylamide/bis, ammonium persulfate, TEMED, PVDF membranes, and enhanced chemiluminescence reagents) were purchased from sources as described previously (Paine *et al.*, 2005). Baculovirus-insect cell-expressed human CYP3A4 and CYP3A5 (co-expressed with cytochrome P450 reductase but not cytochrome b_5), the anti-CYP3A4 and -CYP3A5 antibodies (WB-3A4 and -3A5, respectively), and 1'-hydroxymidazolam (1'-OH MDZ) were purchased from BD Gentest (Woburn, MA). A panel of 10 African American liver microsomal preparations (race/ethnicity supplied by the manufacturer) was purchased from Xenotech, LLC (Lenexa, KS). The secondary antibody, goat anti-rabbit horseradish peroxidase-conjugated IgG, was purchased from Zymed Laboratories (South San Francisco, CA). Midazolam maleate, alprazolam, erythromycin, and NADPH were purchased from Sigma-Aldrich (St. Louis, MO). Fluconazole was purchased from MP Biomedicals (Irvine, CA). $^{15}N_3$-midazolam was a gift from Hoffman-La Roche (Nutley, NJ). [^{14}C *N*-methyl]erythromycin (specific activity, 48.8 mCi/mmol; radiochemical purity, 98.8%) was purchased from PerkinElmer (Shelton, CT). [^{3}H]Formaldehyde (specific activity, 20 Ci/mmol; radiochemical purity, 99%) was purchased from American Radiolabeled Chemicals (St. Louis, MO). All other chemicals were of electrophoresis or analytical grade where appropriate.

Characterization of Human Liver Microsomes for CYP3A Protein Content and Susceptibility to Inhibition

Western blot analysis for CYP3A content. A panel of liver microsomes obtained from African American donors (n = 10) was characterized as described previously (Lyke *et al.*, 2003) to generate two pools of HLM that contained either CYP3A4 or CYP3A5 as the major CYP3A enzyme. Briefly, microsomes were diluted in sample buffer as described (Paine *et al.*, 2005) to yield a final concentration of 5-20 µg per 60 µl. Reference standards were prepared similarly

using the recombinant CYP3A enzymes (rCYP3As). The diluted microsomal preparations and reference standards were boiled (3 minutes), loaded onto 0.1% SDS-9% polyacrylamide gels (14 x 16 cm), and the proteins were separated by electrophoresis as described previously (Paine *et al.*, 2005). The proteins were transferred overnight to PVDF membranes at 4°C, after which the membranes were placed in blocking buffer [5% nonfat dry milk in phosphate buffered saline containing 0.3% Tween 20 (PBS-T)] at room temperature. After 1 hour, the blots were rinsed in PBS-T, then incubated with the anti-CYP3A4 (1:500) or anti-CYP3A5 (1:3000) antibody. After 1 (anti-CYP3A4) or 2 (anti-CYP3A5) hours, the membranes were rinsed in PBS-T, incubated with the secondary antibody (1:500 x 1 hour for CYP3A4; 1:3000 x 2 hours for CYP3A5), and rinsed again. The proteins of interest were visualized by enhanced chemiluminescence using the Chemi-Doc imaging system (Bio-Rad, Hercules, CA). Integrated optical densities (IODs) were obtained using the Bio-Rad software program Quantity One (version 4.1). Calibration curves were generated by plotting the IODs of the reference standards against the mass of rCYP3A loaded. The amount of CYP3A enzyme/well was calculated relative to the calibration curve. Specific content was calculated by dividing the amount of enzyme/well by the amount of total microsomal protein loaded. The three preparations with undetectable CYP3A5 were pooled and designated as "CYP3A5 nonexpressors". The three preparations with the highest percent CYP3A5 content (with respect to total CYP3A content, CYP3A4+CYP3A5) were pooled and designated as "CYP3A5 expressors". Each pool was then analyzed for CYP3A4 and CYP3A5 content in the same manner as described for the individual preparations.

Inhibitory potency of fluconazole towards CYP3A catalytic activity. The inhibitory potency of fluconazole towards CYP3A activity (midazolam 1'-hydroxylation or erythromycin *N*-demethylation) was evaluated using the CYP3A5- and CYP3A5+ HLM. For comparison, similar experiments were conducted with rCYP3As. Midazolam and fluconazole were dissolved in methanol to yield concentrated solutions ranging from 1-8 mM and 0.5-40 mM, respectively.

Erythromycin was dissolved in methanol to yield a 10 mM solution. To increase the sensitivity of the radiometric assay for determination of erythromycin N-demethylase activity (Lyke *et al.*, 2003), [^{14}C]erythromycin was purified to remove trace amounts of [^{14}C]formaldehyde. In brief, a volume of the stock solution (in 100% ethanol) was diluted 1:10 in water, after which a saturated solution of sodium carbonate (0.5% v/v) was added. The diluted solution was then loaded onto a pre-equilibrated C_{18} Bond Elute cartridge (Varian Inc., Palo Alto, CA), and the impurities were eluted with 10% methanol. The cartridge was allowed to dry, and the purified [^{14}C]erythromycin was eluted with 100% methanol. The volume of purified [^{14}C]erythromycin was then adjusted with 100% methanol to achieve a radioactivity concentration of ~2 µCi/ml.

K_i of fluconazole using midazolam as substrate. Reaction mixtures consisted of 0.05 mg/ml microsomal protein or 20 pmol/ml rCYP3A, midazolam (1-8 µM), fluconazole (0-80 or 0-400 µM), and potassium phosphate buffer (0.1 M, pH 7.4). After a 5-minute equilibration period at 37°C, the reactions were initiated with NADPH (final concentration, 1 mM) to yield a final volume of 0.5 ml. Reactions were quenched after 2 (microsomes) or 4 (rCYP3A) minutes with 1 ml ice-cold acetonitrile. The resulting mixtures were spiked with internal standard (alprazolam, 30 pmol), vortex-mixed, and stored at -20°C pending analysis for 1'-OH MDZ by liquid chromatography/mass spectrometry as described previously (Paine *et al.*, 2004). The amount of 1'-OH MDZ formed was linear with respect to the incubation time and amount of enzyme source. Initial estimates of the apparent K_m and V_{max} were derived from Eadie-Hofstee plots of the substrate concentration-velocity data in the absence of inhibitor. Initial estimates of the apparent K_i were derived from Dixon plots of the inhibitor concentration-velocity data. Kinetic parameters (K_m, V_{max}, K_i) were obtained from untransformed data by nonlinear least-squares regression using WinNonlin (v4.1, Pharsight, Mountain View, CA). The appropriateness of the model (competitive, noncompetitive, or mixed-type inhibition for a unienzyme system) was assessed from visual inspection of the observed *vs.* predicted data, randomness of the

residuals, Akaike information criteria, and standard errors of the parameter estimates. Apparent intrinsic clearance (Cl_{int}) was calculated as the ratio of V_{max} to K_m.

IC_{50} of fluconazole using ^{14}C-erythromycin as substrate. For technical and cost reasons, the IC_{50}, rather than K_i, was determined. The highly sensitive radiometric assay for the determination of erythromycin *N*-demethylase activity has been described previously (Lyke *et al.*, 2003) and was modified from a method by Riley and Howbrook (1997). The amount of [^{14}C]erythromycin required for an experiment (*i.e.*, 0.2 µCi/incubation) was removed from the diluted purified stock solution and combined with an appropriate volume of the cold erythromycin solution (10 mM) to achieve a total erythromycin content of 10 nmol/incubation. This batch substrate mix was evaporated to dryness under nitrogen and solubilized in 1 µl methanol/incubation. Potassium phosphate buffer (0.1 M, pH 7.4) was then added to achieve a concentration of 10 nmol erythromycin/50 µl, and the mixture was chilled on ice before adding to the reaction tubes. Reaction mixtures consisted of 0.125 mg/ml microsomal protein or 50 pmol/ml rCYP3A, erythromycin (50 µM, which approximates the K_m), fluconazole (0-400 µM), and potassium phosphate buffer. After a 5-minute equilibration period at 37°C, the reactions were initiated with NADPH (final concentration, 1 mM) to yield a final volume of 0.2 ml. Reactions were quenched after 10 minutes with 50 µl of 10% trichloroacetic acid and placed on ice. The mixtures were spiked with 50 µl of internal standard (consisting of 0.05 µCi/ml [^{3}H]formaldehyde with 0.06 M cold formaldehyde and 0.5 mM cold erythromycin as trace carriers) and centrifuged, and the supernatants were transferred to pre-equilibrated Supelclean Envi-Carb solid phase extraction tubes (3 ml, 0.25 g) (Sigma-Aldrich). The tubes were eluted with 2 volumes of water (2 × 0.5 ml), which was transferred to scintillation vials containing 20 ml scintillation cocktail. The vials were placed in a PerkinElmer TRI-carb 2900T liquid scintillation analyzer, and the radioactivity was counted using a dual ^{3}H/^{14}C program (QuantaSmart 1.1 software, PerkinElmer). The amount of [^{14}C]formaldehyde formed was linear with respect to the

incubation time and amount of enzyme source. Percent control activity was determined as the ratio of the amount of $[^{14}C]$formaldehyde formed in the presence to that in the absence of fluconazole. Initial estimates of the apparent IC_{50} were derived from linear regression of the natural logarithm of [fluconazole] *vs.* percent control activity data. The apparent IC_{50} was obtained from untransformed data by nonlinear least-squares regression using WinNonlin.

Human Volunteer Study

Subjects. All subjects provided written, informed consent before participating in the clinical protocol, which was approved by the Institutional Review Board and the Clinical Research Advisory Committee at the University of North Carolina. To maximize the probability of identifying homozygous *CYP3A5*1* carriers, only African American subjects were recruited. Healthy unrelated volunteers, self-identified as African American or Black, provided mouthwash samples, from which genomic DNA was isolated using the QIAamp® DNA blood mini kit (QIAGEN Inc., Valencia, CA). Roughly equal numbers of volunteers genotyped as *CYP3A5*1/*1* (n = 6), "*CYP3A5*1/*X*" (n = 7), or "*CYP3A5*X/*X*" (n = 6) were enrolled in the pharmacokinetic study; in this context, "*X*" represents the *CYP3A5*3, *6* or *7* allele. Individuals carrying two *CYP3A5*1* alleles (*CYP3A5*1/*1*), or one *CYP3A5*1* allele (*CYP3A5*1/*X*), were designated as CYP3A5 expressors. Individuals with two copies of the same defective allele (*CYP3A5*X/*X*) were designated as CYP3A5 nonexpressors. Individuals with two different defective alleles (*CYP3A5*3/*6, CYP3A5*3/*7*, or *CYP3A5*6/*7*) were excluded to avoid potential inference about the phenotype.

The participants, 13 women and 6 men, ranged in age from 18 to 45 years (average ± SD, 24 ± 8 years) and in weight from 57 to 97 kg (average ± SD, 76 ± 12 kg). Prior to enrollment, each subject presented for a screening visit that consisted of a medical history, physical examination, vital signs, and laboratory tests that included a complete blood count and blood chemistries (BUN, serum creatinine, AST, ALT, alkaline phosphatase, total bilirubin). All

of the women underwent a serum pregnancy test. None of the subjects was taking medications, prescription or non-prescription (including herbal products), known to alter CYP3A activity. All subjects were instructed to refrain from consuming grapefruit-containing products beginning at least one week before and during the course of the study, as well as to refrain from caffeinated and alcoholic beverages the evening before admission to the UNC General Clinical Research Center (GCRC).

Determination of CYP3A5 genotype. CYP3A5 genotype was determined based on sequencing assays for the *CYP3A5*3* (Kuehl *et al.*, 2001), *CYP3A5*6* (14690G>A), and *CYP3A5*7* (27131-32insT) variant alleles. PCR for *CYP3A5*6* genotyping was performed using forward *(5'-TTGCTGCATGTATAGTGGAAGG-3')* and reverse *(5'-GTGTGAGGGCTCTAGATTGACA-3')* primers at concentrations of 400 nM, 50 ng of template DNA, and Ready-to-Go bead (puReTaq Ready-to-Go PCR beads, Amersham Biosciences) in a final volume of 25 µl, producing a 419-bp fragment of the *CYP3A5* gene. A 461-bp amplicon was obtained by identical conditions for *CYP3A5*7* genotyping using forward *(5'-CTCCTCCACACATCTCAGTAGGT-3')* and reverse (5'-CATTTCCCTGGAGACTTGTACC-3') primers. PCR amplification consisted of the following: after an initial denaturing step at 95°C for 5 min, amplification was performed for 35 cycles of denaturation (95°C for 30 s), annealing (55°C for 30 s), and extension (72°C for 60 s), followed by a final extension at 72°C for 5 min. PCR products were spin column-purified to remove unincorporated nucleotides and primers using the QIAquick® PCR Purification Kit (QIAGEN Inc.) and sequenced for the forward and reverse direction on an ABI Prism 377Xl DNA Sequencer (Applied Biosystems, Foster City, CA) with the ABI Prism® BigDye™ Terminator Cycle Sequencing Ready Reaction Kit (PerkinElmer).

Study design. The clinical protocol consisted of two study phases scheduled on consecutive days. Subjects were admitted to the GCRC the evening before the first phase. All of the women underwent a repeat serum pregnancy test prior to initiation of other study procedures. All subjects underwent an overnight fast before each study phase. On the morning

of the first phase (day 1), an indwelling heparin-lock catheter was placed into an antecubital vein

for serial blood collections and for administration of the erythromycin breath test (ERMBT) as

described (Paine *et al.*, 2002). In brief, 3 µCi (0.07 µmol) of [^{14}C *N*-methyl]erythromycin

(Metabolic Solutions, Nashua, NH) were diluted in 5 ml of 5% dextrose and given over one

minute. Prior to and 20 minutes after injection, the subject exhaled into a collection bag through

a Quintron (Milwaukee, WI) disposable modified Haldane-Priestley tube. After injection of [^{14}C

N-methyl]erythromycin, a med-lock was placed into the opposite antecubital vein for

administration of midazolam (1 mg) (Bedford Laboratories, Bedford, OH). Midazolam was given

30 minutes after [^{14}C *N*-methyl]erythromycin injection, then the med-lock was discontinued.

Blood (5 ml) was drawn through the indwelling catheter into EDTA-containing Vacutainer tubes

(Becton-Dickinson, Rutherford, NJ) just before midazolam administration and 5, 10, 15, 45, 60,

120, 180, 240, 360, 480, 600, and 720 minutes thereafter. Plasma was separated from blood

cells by centrifugation (3500 $\times$ *g*, 15 min, 4°C) and stored at -80°C pending analysis for

midazolam.

The second study phase (day 2) began the following morning, when the subject was

given a single oral dose (400 mg) of fluconazole (Diflucan®, Pfizer, New York, NY). Ninety

minutes after fluconazole was given, the ERMBT was administered (at approximately the same

time as on the previous day). Midazolam was given 30 minutes after [^{14}C *N*-

methyl]erythromycin injection (*i.e.*, 120 minutes after fluconazole). Blood (10 ml) was collected

through the indwelling catheter just before fluconazole administration, just before midazolam

administration, and at 5, 10, 15, 45, 60, 120, 180, 240, 360, 480, 600, and 720 minutes after

midazolam administration. Plasma was separated from blood cells by centrifugation (3500 $\times$ *g*,

15 min, 4°C) and stored at -80°C pending analysis for fluconazole and midazolam. During both

study phases, meals and snacks, which were devoid of grapefruit-containing products and

caffeinated beverages, were provided after the 240-minute (4-hour) blood collection with respect

to midazolam administration. Vital signs (blood pressure, pulse, respirations, temperature) were monitored periodically until the last blood collection, after which the subject was discharged.

Analytic Procedures

$^{14}CO_2$ in breath following ERMBT administration. The collected breath was bubbled, *via* a peristaltic pump, into a scintillation vial containing 4 ml of a CO_2 trapping solution (benzathonium hydroxide:absolute ethanol, 1:1) and the blue indicator dye, thymolphthalein (1%). When 2 mmol of CO_2 became trapped, as indicated when the blue dye turned clear, scintillation fluid (10 ml) was added, and ^{14}C specific activity was measured by scintillation counting. Results were expressed as the percentage of administered ^{14}C exhaled over the first hour post-injection, as estimated by a single breath collection at 20 minutes (Wagner, 1998).

Midazolam in plasma following intravenous administration. A 0.5-ml aliquot of plasma was diluted with 0.5 ml nanopure water, after which 50 µl of internal standard ($^{15}N_3$-midazolam, 1 µg/ml in methanol) were added. After adding 1 ml of saturated sodium borate (pH 10), the mixture was extracted with 5 ml of toluene:methylene chloride (7:3), shaken for 20 min, and centrifuged ($900 \times g$, 20 min). The organic layer was collected and evaporated to dryness under nitrogen at 47°C. The residues were reconstituted with 50 µl of methanol, vortex-mixed gently, and then transferred to HPLC vials containing 50 µl of nanopure water. A 10-µl aliquot was injected onto an HPLC system consisting of a Shimadzu (Columbia, MD) LC-10AD pump, DGU-14A degasser, SCL-10A controller, and SIL-10AD autosampler. The HPLC system was coupled to a Micromass Quattro II triple quadrupole mass spectrometer (Manchester, UK) operated in the positive ion electrospray atmospheric pressure ionization mode. Analytes were separated with a Zorbax Eclipse XDB-C8 column (5 µm, 2.1 mm $\times$ 50 mm) (Agilent Technologies, Palo Alto, CA) equipped with a Phenomenex SecurityGuard C8 guard column (Torrance, CA). The mobile phase, at a flow rate of 0.3 ml/min, consisted initially of 45% methanol/water and 0.1% acetic acid. After 0.5 min, methanol was increased linearly to 60%

over 1.5 min, held for 0.5 min, increased to 90% over 0.5 min, held for 5 min, then decreased

back to 45% and held for 2 min. Ions with *m/z* ratios of 325.9 and 328.9 were monitored for

midazolam and $^{15}N_3$-midazolam, respectively. Midazolam was quantified by comparing peak

area ratios (midazolam/$^{15}N_3$-midazolam) to those from a standard curve prepared with known

amounts of midazolam using Micromass Masslynx data analysis software. The inter-day

coefficient of variation in the assay was 6.7% and 5.0% at 2 ng/ml and 50 ng/ml midazolam,

respectively.

Fluconazole in plasma following oral administration. Perchloric acid:water (1:1) (15

μl) was added to plasma (0.2 ml), on ice, and the mixtures were vortex-mixed and centrifuged

(15,000 × *g* for 10 min at 4°C). The supernatant (115 μl) was transferred to microfuge tubes

containing 24 μl of potassium phosphate buffer (2 M, pH 12), vortex-mixed, kept on ice for 40

minutes, then centrifuged (15,000 × *g* for 10 min at 4°C). The supernatant was transferred to

HPLC vials, and 25 μl were injected onto the HPLC system, which consisted of a Hewlett

Packard series 1050 UV detector and autosampler and an Agilent series 1100 pump and

degasser. Fluconazole was eluted using an Eclipse XDB-C8 column (5 μm, 4.6 × 150 mm).

Mobile phase A consisted of 40% methanol/40% acetonitrile/20% water, and mobile phase B

consisted of 40% methanol/60% water. The initial conditions were 100% B at a flow rate of 0.7

ml/min, followed by a linear gradient to 100% A over 8 minutes. At 9 minutes, the flow rate was

increased to 1.4 ml/min and held for 13 minutes, after which the flow rate was returned to 0.7

ml/min and 100% B over 1 minute. Fluconazole was detected by UV absorbance at 260 nm.

The interday variation in the assay was 3.4% at 5.5 μg/ml.

Pharmacokinetic Analysis and *In Vitro – In Vivo* Prediction of CYP3A Inhibition.

The pharmacokinetics of midazolam were evaluated using a noncompartmental approach

(WinNonlin). The area under the plasma concentration *vs*. time curve (AUC) was determined

using the log-linear trapezoidal method, and systemic clearance (Cl) was calculated as the ratio

of dose to AUC. The terminal elimination half-life was obtained from the linear terminal slope of the semilog plot. The *in vivo* K_i ($K_{i,iv}$) for the inhibition of midazolam metabolism by fluconazole was calculated according to the following equation (Tucker, 1992; Yao *et al.*, 2003):

$$\frac{Cl_{int,c}}{Cl_{int,i}} = \frac{1}{\left(\dfrac{f_m}{1+\left(\dfrac{[I]}{K_{i,iv}}\right)}\right)+(1-f_m)} \tag{1}$$

where $Cl_{int,i}$ and $Cl_{int,c}$ denote the intrinsic clearance of the substrate under inhibited and control conditions, respectively; f_m denotes the fraction of the clearance mediated by the inhibited pathway; $[I]$ denotes the average plasma concentration of the inhibitor (competitive or non-competitive); and $K_{i,iv}$ is the *in vivo* K_i. If midazolam is assumed to be metabolized entirely by a single enzyme (*i.e.*, $f_m = 1$), equation 1 simplifies to:

$$\frac{Cl_{int,c}}{Cl_{int,i}} = 1 + \frac{[I]}{[K_{i,iv}]} \tag{2}$$

The average inhibitor concentration after midazolam administration was calculated as $AUC_{120-840min}/720$ min. The high unbound fraction of fluconazole in plasma (~89%) was not considered in the calculation. $Cl_{int,c}$ and $Cl_{int,i}$ were determined by rearrangement of the well-stirred model for hepatic clearance:

$$Cl_{int} = \frac{Q_p \times Cl}{f_u \times (Q_p - Cl)} \tag{3}$$

where Q_p and f_u denote hepatic plasma flow and the plasma unbound fraction of midazolam (0.02), respectively. Q_p was calculated using the measured hematocrit (Hcr) for each subject and the following equation: (0.02 l/min/kg $\times$ subject weight) $\times$ (1-Hcr). In addition, the mean intrinsic clearance in each genotype group was calculated from the mean blood clearance after conversion of plasma clearance to blood clearance using a midazolam blood-to-plasma ratio of

16

0.6 (Gorski *et al.*, 1998). Equation 2 was also used to determine the $K_{i,iv}$ of fluconazole towards the ERMBT, assuming erythromycin *N*-demethylation is mediated exclusively by CYP3A (McGinnity *et al.*, 1999) and that the $ERMBT_c/ERMBT_i$ ratio approximates the blood $Cl_{int,c}/Cl_{int,i}$ ratio for the *N*-demethylation pathway. The inhibitor concentration at the end of the 20-min breath collection period (*i.e.*, 110 min after the fluconazole dose) was used in the calculation. The ratio of *in vitro*/*in vivo* K_i values, RK_i, was calculated from each set (midazolam and erythromycin) of experimentally derived inhibition parameters. For erythromycin, the *in vitro* K_i was assumed to be equal to the IC_{50} for a non-competitive inhibition mechanism (Kenworthy *et al.*, 1999), which was based on inhibition data involving fluconazole and the related CYP3A substrate cyclosporine (Omar *et al.*, 1997).

Statistical Analysis

The *in vitro* enzyme kinetic values are presented as means ± SEs of the parameter estimates. All statistical comparisons were made using SAS (version 9.1, SAS Institute Inc., Cary, NC). The associations between *CYP3A5* genotype and the following four outcomes were assessed by regression analysis: inhibition of midazolam clearance by fluconazole, inhibition of the ERMBT by fluconazole, the $K_{i,iv}$ of fluconazole towards midazolam, and the $K_{i,iv}$ of fluconazole towards the ERMBT. To stabilize the variance in the outcomes and satisfy the statistical assumptions required for ANOVA, the logarithm of each outcome was used as the dependent variable. The assumptions of normality and homoscedasticity were verified from residual plots; with all datasets, no evidence was found that contradicted model assumptions. The midazolam AUC and the ERMBT were adjusted for the logarithm of control values in order to appropriately account for baseline differences in these variables among subjects. Relationships between midazolam Cl and the ERMBT under control and inhibited conditions were evaluated from Spearman correlation coefficients (r_s). For all analyses, a *p*-value <0.05 was considered significant.

17

RESULTS

Specific CYP3A4 and CYP3A5 content in pooled human liver microsomes. Based on the specific contents of CYP3A4 and CYP3A5 in the individual liver microsomal preparations (data not shown), the pooled preparation designated as CYP3A5 expressors (CYP3A5+) contained a low amount, while the pool designated as CYP3A5 non-expressors (CYP3A5-) contained a high amount, of CYP3A4 immunoreactive protein (Fig. 1). Conversely, the CYP3A5+ HLM contained a high amount, whereas the CYP3A5- HLM contained essentially no detectable CYP3A5 immunoreactive protein. Specific protein content in each pair of replicates varied <15%. CYP3A4 and CYP3A5 content in the CYP3A5+ HLM averaged 13 and 58 pmol/mg, respectively; CYP3A4 content in the CYP3A5- HLM averaged 133 pmol/mg. Accordingly, CYP3A5 represented 82% and 0% of total CYP3A (CYP3A4+CYP3A5) content in the CYP3A5+ and CYP3A5- HLM, respectively.

Inhibition kinetics of fluconazole toward CYP3A catalytic activity. With midazolam as the substrate, and in the absence of fluconazole, 1'-OH MDZ formation by each pool of HLM was consistent with classic Michaelis-Menten kinetics for a unienzyme system, as exemplified from linear, monophasic Eadie-Hofstee plots (data not shown). Despite the contribution of CYP3A5 to midazolam 1'-hydroxylation, monophasic plots were evident for both HLM pools because CYP3A4 and CYP3A5 exhibit similar K_m values for midazolam 1'-hydroxylation (Gibbs *et al.*, 1999). The apparent K_m and V_{max} values for 1'-OH MDZ formation were similar between the two pools (2.7 ± 0.2 µM and 2.2 ± 0.08 nmol/min/mg, respectively, for the CYP3A5- HLM; 2.9 ± 0.2 µM and 2.9 ± 0.1 nmol/min/mg, respectively, for the CYP3A5+ HLM). The Cl_{int} was therefore similar between the two pools (0.8 and 1.0 µl/min/mg for the CYP3A5- and CYP3A5+ HLM, respectively). For both HLMs, the simple noncompetitive inhibition model best described the fluconazole-midazolam interaction. The K_i of fluconazole was slightly higher in the CYP3A5+ compared to the CYP3A5- HLM (Fig. 2 and Table 1).

1'-OH MDZ formation by each rCYP3A was consistent with classic Michaelis-Menten kinetics for a unienzyme system, and the simple linear mixed-type (rCYP3A4) or competitive (rCYP3A5) inhibition model best described the data. The K_m and V_{max} values obtained from rCYP3A5 were approximately 2.5-fold higher than those obtained from rCYP3A4 (0.9 ± 0.1 μM and 1.7 ± 0.1 pmol/min/pmol, respectively, for rCYP3A4; 2.4 ± 0.2 μM and 5.3 ± 0.1 pmol/min/pmol, respectively, for rCYP3A5). The corresponding Cl_{int} values were therefore similar between the two enzymes (2.0 and 2.2 μl/min/pmol for rCYP3A4 and rCYP3A5, respectively). The K_i obtained from rCYP3A5 was approximately eightfold higher than that obtained from rCYP3A4 (Table 1), consistent with the previous report (Gibbs *et al.*, 1999). The K_is obtained from the rCYP3As were roughly concordant (within 2-fold) with the corresponding values obtained from HLM.

With erythromycin as the substrate, the IC_{50} for fluconazole was slightly lower in the CYP3A5+ HLM compared to the CYP3A5- HLM (Fig. 3, Table 1). In contrast, the IC_{50} obtained from rCYP3A5 was 3.5 times higher than that obtained from rCYP3A4 (Table 1). The IC_{50} obtained from rCYP3A4 was similar to that with CYP3A5- HLM, while the IC_{50} obtained from rCYP3A5 was 6.5-fold higher than that obtained from CYP3A5+ HLM (Table 1).

Influence of CYP3A5 genotype on the extent of inhibition of CYP3A activity in healthy volunteers. To assess whether CYP3A5 expression influences the extent of CYP3A inhibition by fluconazole *in vivo*, a human volunteer study was conducted utilizing the same CYP3A probes. Because both probe drugs were given intravenously, the interaction with fluconazole was assumed to reflect primarily inhibition of hepatic CYP3A.

Fluconazole was rapidly absorbed, reaching a peak concentration within 2-3 hrs after oral administration. Importantly, because midazolam and the ERMBT were administered 1.5-2 hrs after fluconazole was administered, the fluconazole concentration was near or at its peak at the time the CYP3A probes were given (Fig. 4). With midazolam as the probe, in the absence of fluconazole, the AUC and Cl of midazolam were similar among the three genotypic groups

19

(Table 2) (p > 0.05). In the presence of fluconazole, the AUC of midazolam was significantly increased within each group (p < 0.0001); the percent increase was slightly greater in the *CYP3A5*X/*X* group (49 ± 3%) compared to *CYP3A5*1* carriers (36 ± 15% and 40 ± 5% in the *CYP3A5*1/*1* and *CYP3A5*1/*X* groups, respectively) (Table 2, Fig. 4). Correspondingly, midazolam Cl was significantly decreased by fluconazole within each genotypic group (p < 0.001), with the percent decrease being greatest in the *CYP3A5*1* non-carriers (Table 2). The mean $K_{i,iv}$ for fluconazole towards midazolam differed significantly among the three genotypic groups (p = 0.02), with the highest $K_{i,iv}$ observed in the *CYP3A5*1/*1* group (Fig. 5A). The mean (± SD) $K_{i,iv}$ for the *1/*1*, *1/*X*, and *X/*X* groups were 24 ± 17 µM, 17 ± 8 µM, and 13 ± 6 µM, respectively. When the average blood clearance data were used, the corresponding $K_{i,iv}$ values were 21, 20 and 16 µM in the three genotype groups, respectively, demonstrating a similar genotype effect as observed using the plasma clearance.

With the ERMBT as the probe, complete data sets were not available for two of the volunteers in the *1/*X* group. In the absence of fluconazole, the mean (± SD) ERMBT results were 2.40 ± 0.49, 1.95 ± 0.45, and 2.54 ± 0.76 for the *1/*1*, *1/*X*, and *X/*X* group, respectively. The mean values for each group were not significantly different from each other (p > 0.05). In the presence of fluconazole, the mean ERMBT result was significantly decreased (p < 0.05) in all groups (to 1.32 ± 0.19, 1.49 ± 0.27, and 1.48 ± 0.60, respectively), but the extent of inhibition did not differ among the three groups (p = 0.14). Likewise, the corresponding $K_{i,iv}$s did not differ among the groups (p = 0.49) (Fig. 5B). The mean (± SD) $K_{i,iv}$ for the *1/*1*, *1/*X*, and *X/*X* group was 30 ± 12 µM, 77 ± 72 µM, and 58 ± 53 µM, respectively. As has been reported previously (Kinirons *et al.*, 1999; Masica *et al.*, 2004), a correlation was not evident between midazolam Cl (whether normalized to body weight) and the ERMBT, in both the presence and absence of fluconazole (r_s ≤ 0.27, p ≥ 0.28).

20

In Vitro-In Vivo **Extrapolations**. Results from HLM and the *in vivo* study were used to calculate RK_i values for the inhibition of midazolam intrinsic metabolic clearance and the ERMBT by fluconazole. Assuming that the *CYP3A5*1/*1* group had the highest hepatic CYP3A5 content, coupled with the incomplete set of ERMBT values for the *CYP3A5*1/*X* group, only the **1/*1* group was used as the *in vivo* correlate to the CYP3A5+ HLM. With midazolam, the RK_i was 1.04 and 1.15 for the CYP3A5+ and CYP3A5- groups, respectively. With erythromycin, the RK_i was 1.8 and 1.2 for the CYP3A5+ and CYP3A5- groups, respectively.

DISCUSSION

A growing body of *in vitro* data has demonstrated that CYP3A5 is less susceptible (more resistant) than CYP3A4 to inhibition by some therapeutic agents (Gibbs *et al.*, 1999; Jones *et al.*, 1999; McConn *et al.*, 2004; Wang Y *et al.*, 2005). Because CYP3A5 can represent a significant portion of total hepatic CYP3A in some individuals (Kuehl *et al.*, 2001; Lin *et al.*, 2002), and *CYP3A5* genotype can significantly influence the disposition of some CYP3A substrates *in vivo* (*e.g.*, saquinavir, tacrolimus, sirolimus, alprazolam) (Andersson *et al.*, 2005; Mouly *et al.*, 2005; Le Meur *et al.*, 2006; Park *et al.*, 2006), differential inhibition of the two major CYP3A isoforms could explain in part the large interindividual variation observed in the extent of CYP3A-mediated drug-drug interactions. Despite the wealth of *in vitro* and *in vivo* data suggesting that CYP3A5 expression can influence the extent of CYP3A inhibition and/or the clearance of some substrates, to our knowledge, there has been no systematic *in vitro-in vivo* evaluation of this clinically relevant issue. Accordingly, using two distinct CYP3A substrates, the inhibitory effects of fluconazole on hepatic CYP3A activity were examined both in pooled HLM with a high or low CYP3A5 protein content and in healthy volunteers with known *CYP3A5* genotype.

The inhibitory potency of fluconazole towards midazolam 1'-hydroxylation in the CYP3A5+ HLM, in which CYP3A5 content was approximately fourfold greater than CYP3A4 content, was slightly less than that in the CYP3A5- HLM (K_is of 25 and 15 μM, respectively). In contrast, a much greater difference was observed between the recombinant enzymes (K_is of 53 and 7 μM for rCYP3A5 and rCYP3A4, respectively). This discrepancy between the two enzyme systems is attributed in part to the CYP3A5+ HLM containing CYP3A4 at an appreciable fraction (20%) of total CYP3A, which attenuated the relative resistance of CYP3A5 to inhibition. A simulation utilizing results with the same recombinant enzymes and with CYP3A5 representing 80% of total CYP3A content predicted a K_i of 60 μM (Gibbs *et al.*, 1999). The additional discrepancy (60 *vs.* 25 μM) could be due to artificial differences in the microenvironment, *e.g.*,

lipid content, P450 reductase levels, and the presence or absence of cytochrome b_5 and other proteins that may influence the binding and effect of a CYP3A inhibitor. Unlike with midazolam, the inhibitory potency of fluconazole towards erythromycin *N*-demethylation in the CYP3A5+ HLM was slightly higher than that in the CYP3A5- HLM (IC_{50}s of 53 and 71 µM, respectively). However, like with midazolam, the inhibitory difference was less profound than that with recombinant enzymes (IC_{50}s of 350 and 100 µM for rCYP3A5 and rCYP3A4, respectively). Assuming that HLM represented the more clinically relevant system, the corresponding data were used to predict the effect of *CYP3A5* genotype on the hepatic CYP3A-mediated interaction between fluconazole and the two probe substrates *in vivo*.

As predicted by HLM, the (inferred) presence of CYP3A5 lowered the inhibitory potency of fluconazole towards midazolam systemic clearance in healthy volunteers. The average $K_{i,iv}$ for homozygous *CYP3A5*1* carriers was 85% higher than that for the noncarriers and was comparable to the ~70% difference observed in HLM. The ratio of the *in vitro* K_i to the $K_{i,iv}$ (RK_i) was at or near unity for both the CYP3A5- and CYP3A5+ groups (1.0 and 1.2, respectively), underscoring the excellent predictability of the midazolam-fluconazole interaction by HLM. The significant effect of *CYP3A5* genotype on the extent of inhibition of midazolam clearance by fluconazole substantiated an earlier study reported by Yu et al. (2004), who observed a similar difference in the extent of inhibition by itraconazole in healthy Korean individuals genotyped as *CYP3A5*1/*1*, **1/*3*, or **3/*3*.

With erythromycin as the probe, the RK_i value was near unity for the CYP3A5- group, but not for the CYP3A5+ group (1.2 *vs.* 1.8). A potential explanation for this moderate *in vitro-in vivo* discrepancy is that the $ERMBT_c/ERMBT_i$ ratio did not accurately reflect the $Cl_{int,c}/Cl_{int,i}$ ratio of erythromycin *N*-demethylation. In addition, the *in vitro* K_i estimated from the IC_{50} may have differed from the true K_i due to the limited IC_{50} dataset. Although the efflux transporter P-gp has been reported as an important determinant of the ERMBT (Kurnik *et al.*, 2006), P-gp is unlikely to contribute to this *in vitro-in vivo* discrepancy, as fluconazole appeared not to alter P-gp

function (Venkatakrishnan *et al.*, 2000). Despite the modest underprediction of the magnitude of the ERMBT-fluconazole interaction, the data did predict the lack of influence of *CYP3A5* genotype on the interaction, substantiating HLM as the preferred enzyme system to predict the inhibitory effect *in vivo*. Indeed, it is virtually impossible to predict the combined inhibitory effect toward CYP3A4 and CYP3A5 *in vivo* using recombinant enzymes because the relative expression of each enzyme varies considerably between individuals (Lamba *et al.*, 2002; Lin *et al.*, 2002), and the intrinsic clearances between the two enzymes for different substrates can vary (Huang *et al.*, 2004; McConn *et al.*, 2004).

Based on the variable expression of CYP3A4 and CYP3A5, and the difference in the inhibitory potency of fluconazole between the two enzymes, a large interindividual variation in the extent of inhibition of affected substrates would be expected *in vivo* in individuals expressing CYP3A5. Results with midazolam support this contention. For example, two of the study participants in the *CYP3A5*1/*1* group appeared more resistant to fluconazole inhibition than others in the group, with a $K_{i,iv}$ (45 µM) that was similar to the K_i obtained with rCYP3A5 (54 µM), suggesting that CYP3A5 was the major CYP3A enzyme expressed in these individuals. Conversely, one participant in this group had a $K_{i,iv}$ near the K_i obtained with rCYP3A4 (7 µM), suggesting that CYP3A4 was the major CYP3A enzyme expressed in this individual despite having the *CYP3A5*1/*1* genotype. Participants with the *CYP3A5*X/*X* genotype exhibited the lowest degree of interindividual variation with respect to the extent of inhibition of midazolam clearance (1.2-fold), which is expected with metabolic contribution from a single dominant CYP3A enzyme in all subjects. The *CYP3A5*1/*1* group showed the highest degree of variation (3.0-fold), whereas the heterozygous group showed intermediate variation (1.5-fold) relative to the two homozygous groups. These observations and the closeness of the RK_I values to unity are consistent with the significant but modest effect of *CYP3A5* genotype on the extent of inhibition of midazolam clearance.

As also predicted by the CYP3A5- HLM, fluconazole was a more potent inhibitor of midazolam clearance than the ERMBT in *CYP3A5*1* noncarriers, as exemplified by the 4.5-fold difference in the respective $K_{i,iv}$ values (13 *vs.* 58 µM), and demonstrating that the potency of a CYP3A inhibitor can be substrate-dependent *in vivo*. Because the two probes were given within 30 minutes of each other, and by the intravenous route (to avoid a significant contribution by intestinal CYP3A), any variation in inhibitor concentrations and/or CYP3A expression levels as a potential source for this substrate difference was minimized. Moreover, the tracer dose of [^{14}C]erythromycin given was too low to cause significant inhibition of CYP3A enzymes. The presence of CYP3A5 attenuated this apparent substrate dependency both *in vitro* and *in vivo*.

Results from the *in vitro-in vivo* extrapolations demonstrated that the more complex *in vitro* system (HLM *vs.* recombinant enzyme) was superior in predicting the magnitude of the *in vivo* interaction and the effect of *CYP3A5* genotype. It follows that human hepatocytes may serve as an even better system to prospectively evaluate potential *in vivo* drug-drug interactions of this nature, as the enzyme microenvironment should be less disturbed during preparation of hepatocytes than during the preparation of HLM. Hepatocytes would also allow testing of the potential contribution of drug transporters to changes in hepatic clearance.

Although the modest effect of CYP3A5 genotype on the extent of inhibition of midazolam clearance by fluconazole is probably not clinically important, a significant clinical effect on the clearance of other CYP3A substrates, especially those with a narrow therapeutic window, cannot be excluded. For example, the clearance of the immunosuppressant tacrolimus has been demonstrated to be significantly influenced by *CYP3A5* genotype (Andersson *et al*., 2005; Thervet *et al*., 2005), and interactions between tacrolimus and fluconazole, as well as other, more potent azole antifungal agents (ketoconazole and itraconazole) have been documented (Venkatakrishnan *et al*., 2000). More recently, the hepatic clearance of the chemotherapeutic agent vincristine was estimated to be 5-fold greater in CYP3A5 high expressors compared to CYP3A5 low expressors based on results from HLM with known CYP3A4 and CYP3A5 content

and *CYP3A5* genotype (Dennison *et al.*, 2007). Whether *CYP3A5* genotype significantly influences the hepatic clearance of vincristine *in vivo*, as well as the extent of inhibition of both tacrolimus and vincristine by fluconazole and other azole antifungals *in vivo*, awaits further investigation.

In summary, the current work demonstrated that the extent of hepatic CYP3A inhibition by fluconazole *in vitro* and *in vivo* varies with substrate and that inheritance of the *CYP3A5*1* allele was significantly associated with reduced CYP3A inhibition by fluconazole with midazolam, but not with erythromycin, as the probe. Based on these *in vitro-in vivo* extrapolations, HLM, rather than recombinant enzymes, appear to be the preferred *in vitro* system for predicting hepatic CYP3A-mediated drug-drug interactions. Additional studies with CYP3A substrates whose metabolism is influenced significantly by *CYP3A5* genotype (*e.g.*, tacrolimus, vincristine), as well as sensitive to inhibition by fluconazole and other CYP3A inhibitors, are warranted to determine the clinical importance of differences in the susceptibility of CYP3A4 and CYP3A5 to inhibition.

REFERENCES

Andersson T, Flockhart DA, Goldstein DB, Huang SM, Kroetz DL, Milos PM, Ratain MJ and Thummel K (2005) Drug-metabolizing enzymes: evidence for clinical utility of pharmacogenomic tests. *Clin Pharmacol Ther* **78:**559-581.

Dennison JB, Jones DR, Renbarger JL and Hall SD (2007) Effect of CYP3A5 expression on vincristine metabolism with human liver microsomes. *J Pharmacol Exp Ther* **321:**553-563.

Gibbs MA, Thummel KE, Shen DD and Kunze KL (1999) Inhibition of cytochrome P-450 3A (CYP3A) in human intestinal and liver microsomes: comparison of Ki values and impact of CYP3A5 expression. *Drug Metab Dispos* **27:**180-187.

Gorski JC, Jones DR, Haehner-Daniels BD, Hamman MA, O'Mara EM, Jr. and Hall SD (1998) The contribution of intestinal and hepatic CYP3A to the interaction between midazolam and clarithromycin. *Clin Pharmacol Ther* **64:**133-143.

Hosea NA, Miller GP and Guengerich FP (2000) Elucidation of distinct ligand binding sites for cytochrome P450 3A4. *Biochemistry* **39:**5929-5939.

Huang W, Lin YS, McConn DJ, 2nd, Calamia JC, Totah RA, Isoherranen N, Glodowski M and Thummel KE (2004) Evidence of significant contribution from CYP3A5 to hepatic drug metabolism. *Drug Metab Dispos* **32:**1434-1445.

Hustert E, Haberl M, Burk O, Wolbold R, He YQ, Klein K, Nuessler AC, Neuhaus P, Klattig J, Eiselt R, Koch I, Zibat A, Brockmoller J, Halpert JR, Zanger UM and Wojnowski L (2001) The genetic determinants of the CYP3A5 polymorphism. *Pharmacogenetics* **11:**773-779.

Jones DR, Gorski JC, Hamman MA, Mayhew BS, Rider S and Hall SD (1999) Diltiazem inhibition of cytochrome P-450 3A activity is due to metabolite intermediate complex formation. *J Pharmacol Exp Ther* **290:**1116-1125.

Kenworthy KE, Bloomer JC, Clarke SE and Houston JB (1999) CYP3A4 drug interactions: correlation of 10 in vitro probe substrates. *Br J Clin Pharmacol* **48:**716-727.

Kinirons MT, O'Shea D, Kim RB, Groopman JD, Thummel KE, Wood AJ and Wilkinson GR (1999) Failure of erythromycin breath test to correlate with midazolam clearance as a probe of cytochrome P4503A. *Clin Pharmacol Ther* **66:**224-231.

Kuehl P, Zhang J, Lin Y, Lamba J, Assem M, Schuetz J, Watkins PB, Daly A, Wrighton SA, Hall SD, Maurel P, Relling M, Brimer C, Yasuda K, Venkataramanan R, Strom S, Thummel K, Boguski MS and Schuetz E (2001) Sequence diversity in CYP3A promoters and characterization of the genetic basis of polymorphic CYP3A5 expression. *Nat Genet* **27:**383-391.

Kurnik D, Wood AJ and Wilkinson GR (2006) The erythromycin breath test reflects P-glycoprotein function independently of cytochrome P450 3A activity. *Clin Pharmacol Ther* **80:**228-234.

Lamba JK, Lin YS, Schuetz EG and Thummel KE (2002) Genetic contribution to variable human CYP3A-mediated metabolism. *Adv Drug Deliv Rev* **54:**1271-1294.

Le Meur Y, Djebli N, Szelag JC, Hoizey G, Toupance O, Rerolle JP and Marquet P (2006) CYP3A5*3 influences sirolimus oral clearance in de novo and stable renal transplant recipients. *Clin Pharmacol Ther* **80:**51-60.

Lin YS, Dowling AL, Quigley SD, Farin FM, Zhang J, Lamba J, Schuetz EG and Thummel KE (2002) Co-regulation of CYP3A4 and CYP3A5 and contribution to hepatic and intestinal midazolam metabolism. *Mol Pharmacol* **62:**162-172.

Lyke AC, Nelsen AC, Paine MF, Rowland EE, Kashuba ADM, Lindley CM, Clarke, M.J. and Hawke RL (2003) Correlation of intrinsic clearance estimates for erythromycin *N*-demethylation (ERMND) and midazolam 1'-hydroxylation (MDZOH) with CYP3A4 and CYP3A5 content using human liver microsomes (HLM). *Clin Pharmacol Ther* **73:**P19.

Masica AL, Mayo G and Wilkinson GR (2004) In vivo comparisons of constitutive cytochrome P450 3A activity assessed by alprazolam, triazolam, and midazolam. *Clin Pharmacol Ther* **76:**341-349.

McConn DJ, 2nd, Lin YS, Allen K, Kunze KL and Thummel KE (2004) Differences in the inhibition of cytochromes P450 3A4 and 3A5 by metabolite-inhibitor complex-forming drugs. *Drug Metab Dispos* **32:**1083-1091.

McGinnity DF, Griffin SJ, Moody GC, Voice M, Hanlon S, Friedberg T and Riley RJ (1999) Rapid characterization of the major drug-metabolizing human hepatic cytochrome P-450 enzymes expressed in Escherichia coli. *Drug Metab Dispos* **27:**1017-1023.

Mouly SJ, Matheny C, Paine MF, Smith G, Lamba J, Lamba V, Pusek SN, Schuetz EG, Stewart PW and Watkins PB (2005) Variation in oral clearance of saquinavir is predicted by CYP3A5*1 genotype but not by enterocyte content of cytochrome P450 3A5. *Clin Pharmacol Ther* **78:**605-618.

Omar G, Whiting PH, Hawksworth GM, Humphrey MJ and Burke MD (1997) Ketoconazole and fluconazole inhibition of the metabolism of cyclosporin A by human liver in vitro. *Ther Drug Monit* **19:**436-445.

Paine MF, Criss AB and Watkins PB (2004) Two major grapefruit juice components differ in intestinal CYP3A4 inhibition kinetic and binding properties. *Drug Metab Dispos* **32:**1146-1153.

Paine MF, Ludington SS, Chen ML, Stewart PW, Huang SM and Watkins PB (2005) Do men and women differ in proximal small intestinal CYP3A or P-glycoprotein expression? *Drug Metab Dispos* **33:**426-433.

Paine MF, Wagner DA, Hoffmaster KA and Watkins PB (2002) Cytochrome P450 3A4 and P-glycoprotein mediate the interaction between an oral erythromycin breath test and rifampin. *Clin Pharmacol Ther* **72:**524-535.

Park JY, Kim KA, Park PW, Lee OJ, Kang DK, Shon JH, Liu KH and Shin JG (2006) Effect of CYP3A5*3 genotype on the pharmacokinetics and pharmacodynamics of alprazolam in healthy subjects. *Clin Pharmacol Ther* **79:**590-599.

Schrag ML and Wienkers LC (2001) Covalent alteration of the CYP3A4 active site: evidence for multiple substrate binding domains. *Arch Biochem Biophys* **391:**49-55.

Stresser DM, Blanchard AP, Turner SD, Erve JC, Dandeneau AA, Miller VP and Crespi CL (2000) Substrate-dependent modulation of CYP3A4 catalytic activity: analysis of 27 test compounds with four fluorometric substrates. *Drug Metab Dispos* **28:**1440-1448.

Thervet E, Legendre C, Beaune P and Anglicheau D (2005) Cytochrome P450 3A polymorphisms and immunosuppressive drugs. *Pharmacogenomics* **6:**37-47.

Tucker GT (1992) The rational selection of drug interaction studies: implications of recent advances in drug metabolism. *Int J Clin Pharmacol Ther Toxicol* **30:**550-553.

Venkatakrishnan K, von Moltke LL and Greenblatt DJ (2000) Effects of the antifungal agents on oxidative drug metabolism: clinical relevance. *Clin Pharmacokinet* **38:**111-180.

Wagner D (1998) CYP3A4 and the erythromycin breath test. *Clin Pharmacol Ther* **64:**129-130.

Wang RW, Newton DJ, Liu N, Atkins WM and Lu AY (2000) Human cytochrome P-450 3A4: in vitro drug-drug interaction patterns are substrate-dependent. *Drug Metab Dispos* **28:**360-366.

Wang YH, Jones DR and Hall SD (2005) Differential mechanism-based inhibition of CYP3A4 and CYP3A5 by verapamil. *Drug Metab Dispos* **33:**664-671.

Wilkinson GR (2005) Drug metabolism and variability among patients in drug response. *N Engl J Med* **352:**2211-2221.

Wojnowski L (2004) Genetics of the variable expression of CYP3A in humans. *Ther Drug Monit* **26:**192-199.

Xie HG, Wood AJ, Kim RB, Stein CM and Wilkinson GR (2004) Genetic variability in CYP3A5 and its possible consequences. *Pharmacogenomics* **5:**243-272.

Yao C, Kunze KL, Trager WF, Kharasch ED and Levy RH (2003) Comparison of in vitro and in vivo inhibition potencies of fluvoxamine toward CYP2C19. *Drug Metab Dispos* **31:**565-571.

Yu KS, Cho JY, Jang IJ, Hong KS, Chung JY, Kim JR, Lim HS, Oh DS, Yi SY, Liu KH, Shin JG and Shin SG (2004) Effect of the CYP3A5 genotype on the pharmacokinetics of intravenous midazolam during inhibited and induced metabolic states. *Clin Pharmacol Ther* **76:**104-112.

Yuan R, Madani S, Wei XX, Reynolds K and Huang SM (2002) Evaluation of cytochrome P450 probe substrates commonly used by the pharmaceutical industry to study in vitro drug interactions. *Drug Metab Dispos* **30:**1311-1319.

FOOTNOTES

Reprint requests: Mary F. Paine

3312 Kerr Hall, CB#7360

School of Pharmacy

The University of North Carolina at Chapel Hill

Chapel Hill, NC 27599-7360

Office: (919) 966-9984

Fax: (919) 962-0644

Email: mpaine@med.unc.edu

LEGENDS FOR FIGURES

Fig. 1. Western blots showing the presence or absence of CYP3A5 immunoreactive protein in the pooled human liver microsomes (HLM) designated as CYP3A5 expressors (E) and nonexpressors (NE). The mass of microsomal protein/lane represents 5 (CYP3A4) or 10 (CYP3A5) µg. Recombinant CYP3A4 and CYP3A5 were used as reference standards. Specific protein content in each pair of replicates varied <15%.

Fig. 2. Dixon plots showing the inhibition of midazolam 1'-hydroxylation by fluconazole in pooled human liver microsomes designated as CYP3A5 nonexpressors (**A**) and CYP3A5 expressors (**B**). Symbols denote the observed data and are means of duplicate incubations. Lines denote the linear regression of the predicted, transformed data. *MDZ,* midazolam.

Fig. 3. IC_{50} determination for fluconazole towards erythromycin *N*-demethylation in pooled human liver microsomes designated as CYP3A5 nonexpressors (**A**) and CYP3A5 expressors (**B**). The concentration of erythromycin was 50 µM, which approximated the K_m. Symbols denote the observed data and are means of duplicate incubations. Lines denote the linear regression of the predicted, transformed data.

Fig. 4. Concentration-time profiles for midazolam (squares) and fluconazole (triangles) in the *CYP3A5*X/*X* (**A**), *CYP3A5*1/*X* (**B**), and *CYP3A5*1/*1* (**C**) groups. Open squares denote midazolam concentrations in the absence of fluconazole; filled squares denote midazolam concentrations in the presence of fluconazole. Fluconazole (400 mg) was given orally 120 minutes before midazolam (1 mg) was administered intravenously. Symbols and error bars denote means and standard deviations, respectively.

Fig. 5. Influence of CYP3A5 genotype on the *in vivo* K_i for fluconazole using midazolam systemic clearance (Cl) (**A**) or the erythromycin breath test (ERMBT) (**B**) as the index of hepatic CYP3A activity. Open squares denote individual values. Closed squares denote the means for each genotypic group. Complete ERMBT data sets were not available for two of the *CYP3A5*1/*X* subjects.

33

TABLE 1

Inhibitory potency of fluconazole towards CYP3A

catalytic activity using midazolam (MDZ) or

erythromycin (ERM) as substrate.

Each value represents the mean ± SE of the

parameter estimate.

Enzyme Source	CYP3A substrate	
	MDZ	*ERM*
Pooled HLM[a]	K_i *(µM)*	IC_{50} *(µM)*
CYP3A5 Nonexpressing	15 ± 0.8	70 ± 2.6
CYP3A5 Expressing	25 ± 1.5	54 ± 1.9
Recombinant Enzyme	K_i *(µM)*	IC_{50} *(µM)*
CYP3A4	7.4 ± 1.9	100 ± 5.3
CYP3A5	53 ± 3.6	350 ± 28

[a]CYP3A5 represented 0% and 82% of total CYP3A

(CYP3A4+CYP3A5) protein content in the CYP3A5

nonexpressing and CYP3A5 expressing HLM,

respectively.

TABLE 2

Pharmacokinetics[a] of midazolam (MDZ) following a single intravenous dose (1 mg), under baseline conditions and under inhibited conditions with a single oral dose (400 mg) of fluconazole (FLUC), in healthy volunteers grouped according to CYP3A5 genotype.

Subject No.	Sex	CYP3A5 Genotype	MDZ AUC (nM-h)		MDZ Cl (L/h)		MDZ t$_{1/2}$ (h)		FLUC C$_{ave}$ (μM)
			Baseline	+FLUC	Baseline	+FLUC	Baseline	+FLUC	
1	M	*1/*1	129	155	23.8	19.8	3.3	2.6	15.2
2	F	*1/*1	126	203	24.8	15.2	5.4	5.1	19.8
3	M	*1/*1	141	174	21.9	17.7	3.3	4.0	15.7
4	F	*1/*1	104	185	29.7	16.7	5.1	6.5	20.8
5	F	*1/*1	149	275	20.6	11.2	5.4	10.3	16.9
6	M	*1/*1	94	195	32.8	15.8	4.2	8.3	16.3
Mean ± SD			*124 ± 21*	*198 ± 41*	*25.6 ± 4.7*	*16.1 ± 2.9*	*4.5 ± 1.0*	*6.1 ± 2.8*	*17.4 ± 2.3*
7	F	*1/*6	109	170	28.3	18.1	5.0	7.9	19.5
8	F	*1/*3	145	213	21.2	14.4	5.9	8.4	19.3
9	F	*1/*6	143	238	21.6	12.9	5.3	6.7	23.0
10	M	*1/*3	133	220	23.2	14.0	2.4	3.2	18.4
11	M	*1/*6	140	236	21.9	13.0	2.5	3.3	19.6
12	F	*1/*3	101	193	30.4	16.0	5.8	5.8	17.5
13	F	*1/*3	76	131	40.6	23.5	2.6	5.4	19.6
Mean ± SD			*121 ± 26*	*200 ± 39*	*26.7 ± 7.1*	*16.0 ± 3.8*	*4.2 ± 1.6*	*5.8 ± 2.1*	*19.5 ± 1.7*
14	F	*3/*3	159	294	19.4	10.5	6.6	7.8	26.9
15	F	*3/*3	94	199	32.6	15.5	3.6	5.1	21.9
16	F	*7/*7	94	195	32.8	15.8	4.2	8.3	21.4
17	M	*3/*3	169	335	18.2	9.2	2.0	2.8	21.8
18	F	*3/*3	104	207	29.5	14.9	2.7	4.3	17.8
19	F	*3/*3	160	293	19.2	10.5	6.9	7.6	25.9
Mean ± SD			*130 ± 36*	*254 ± 61*	*25.3 ± 7.1*	*12.7 ± 3.0*	*4.3 ± 2.0*	*6.0 ± 2.2*	*22.0 ± 6*

[a]*AUC*, area under the concentration *vs.* time curve; *Cl*, systemic clearance; *t$_{1/2}$*, terminal half-life; *C$_{ave}$*, average concentration.
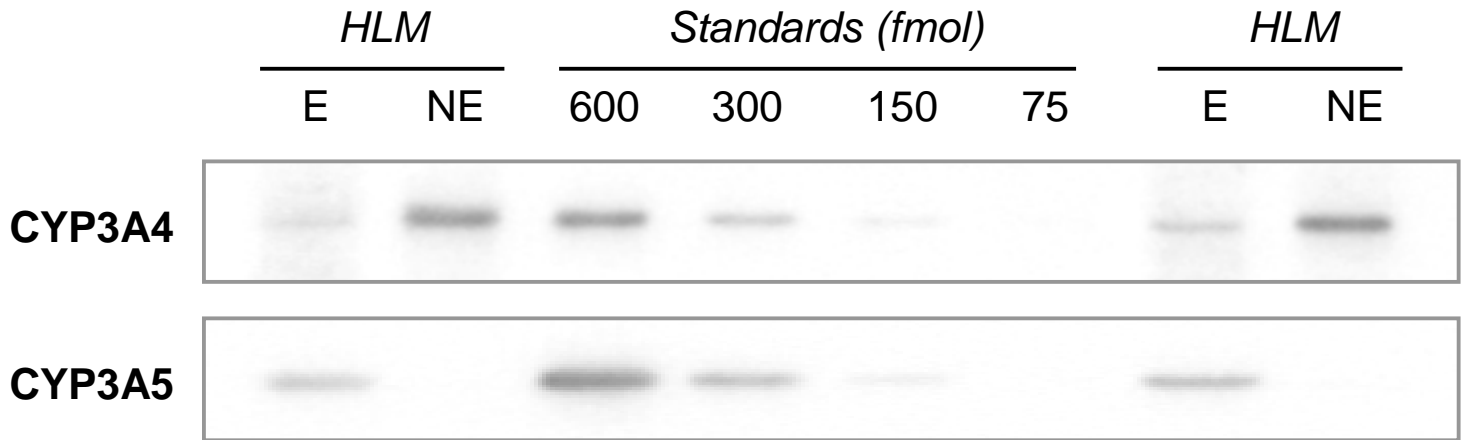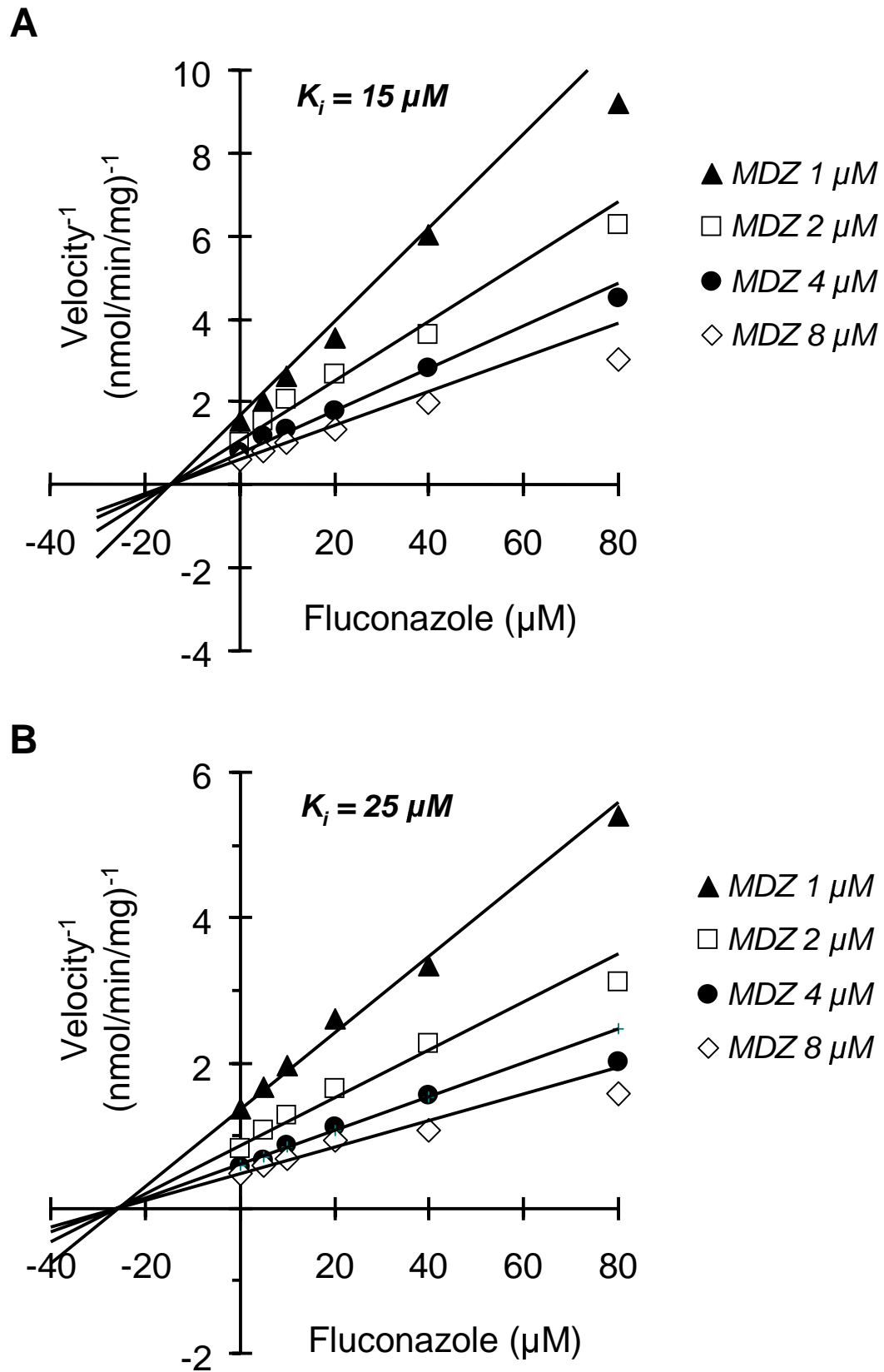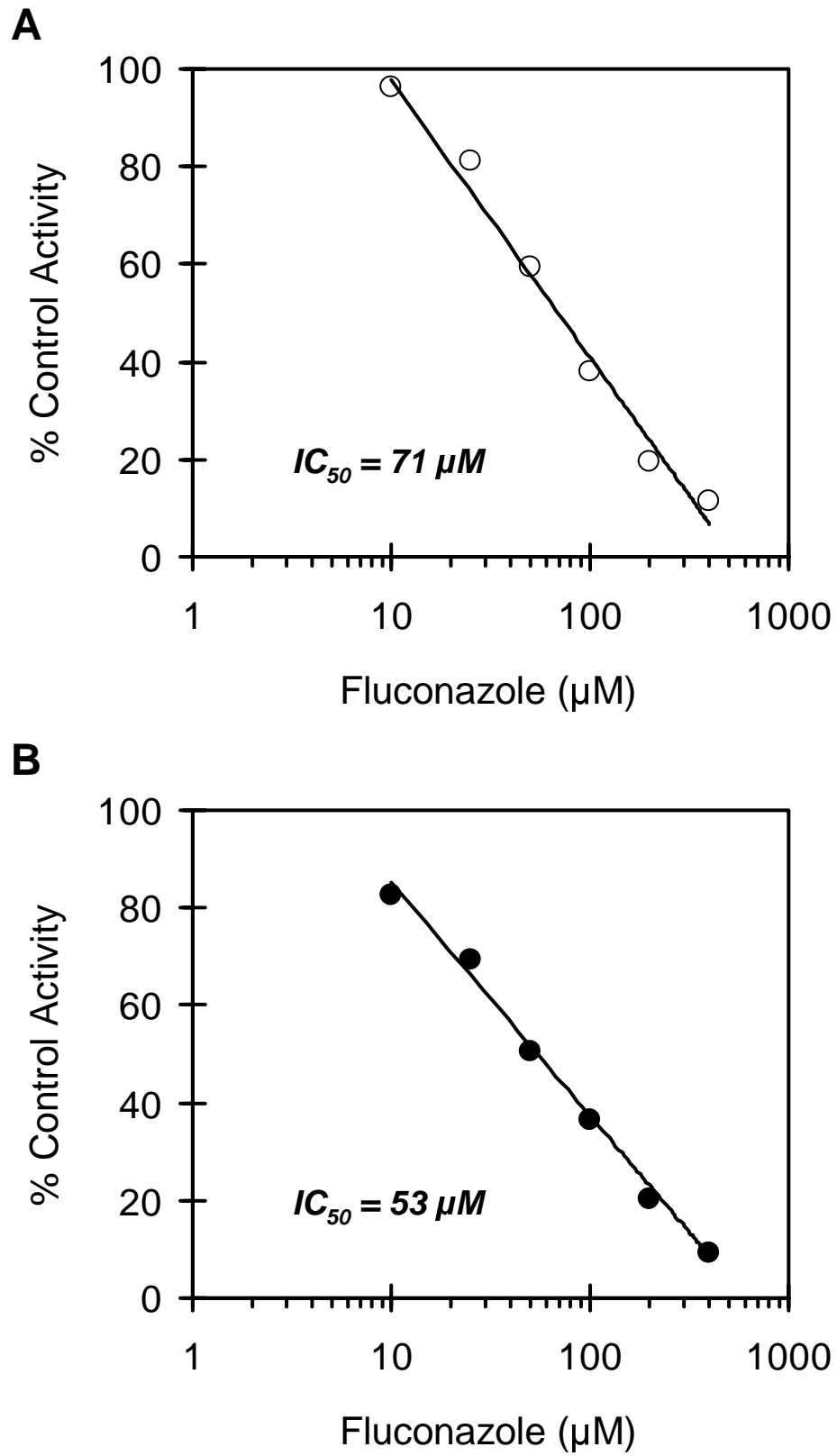
Figure 1

	HLM		*Standards (fmol)*				*HLM*	
	E	NE	600	300	150	75	E	NE
CYP3A4								
CYP3A5								

Figure 2

Figure 3

Figure 4

Figure 5